JOURNAL OF GEOPHYSICAL RESEARCH, VOL. 106, NO. B7, PAGES 13,599–13,611, JULY 10, 2001

Crustal thickness of the Peninsular Ranges and Gulf Extensional Province in the Californias

Jennifer L. Lewis,[1,2] Steven M. Day,[1] Harold Magistrale,[1] Raul R. Castro,[3] Luciana Astiz,[4] Cecilio Rebollar,[3] Jennifer Eakins,[5] Frank L. Vernon,[5] and James N. Brune[6]

Abstract. We estimate crustal thickness along an east-west transect of the Baja California peninsula and Gulf of California, México, and investigate its relationship to surface elevation and crustal extension. We derive Moho depth estimates from *P*-to-*S* converted phases identified on teleseismic recordings at 11 temporary broadband seismic stations deployed at ~31°N latitude. Depth to the Moho is ~33 (±3) km near the Pacific coast of Baja California and increases gradually toward the east, reaching a maximum depth of ~40 (±4) km beneath the western part of the Peninsular Ranges batholith. The crust then thins rapidly under the topographically high eastern Peninsular Ranges and across the Main Gulf Escarpment. Crustal thickness is ~15–18 (±2) km within and on the margins of the Gulf of California. The Moho shallowing beneath the eastern Peninsular Ranges represents an average apparent westward dip of ~25°. This range of Moho depths within the Peninsula Ranges, as well as the sharp ~east-west gradient in depth in the eastern part of the range, is in agreement with earlier observations from north of the international border. The Moho depth variations do not correlate with topography of the eastern batholith. These findings suggest that a steeply dipping Moho is a regional feature beneath the eastern Peninsular Ranges and that a local Airy crustal root does not support the highest elevations. We suggest that Moho shallowing under the eastern Peninsular Ranges reflects extensional deformation of the lower crust in response to adjacent rifting of the Gulf Extensional Province that commenced in the late Cenozoic. Support of the eastern Peninsular Ranges topography may be achieved through a combination of flexural support and lateral density variations in the crust and/or upper mantle.

1. Introduction

Recently, *Ichinose et al*. [1996] and *Lewis et al*. [2000] have shown that the crust-mantle boundary under the Peninsular Ranges batholith in southern California is shallowest under the eastern half of the range where surface elevations are greatest. They proposed that the thinned crust under the eastern Peninsular Ranges reflects extensional deformation of the lower crust in response to rifting in the adjacent Salton Trough. Since the high elevation in the east is not accompanied by local crustal thickening, mantle buoyancy sources and/or lithospheric flexural rigidity probably contribute to the support of the eastern Peninsular Ranges, and these mechanisms may be related to the proximity of the rift margin.

[1]Department of Geological Sciences, San Diego State University, San Diego, California.
[2]Now at Chevron North America Exploration and Production, New Orleans, Louisiana.
[3]División Ciencias de la Tierra, Centro de Investigación Científica y de Educación Superior de Ensenada, Ensenada, Baja California, México.
[4]CTBTO PrepCom, Vienna, Austria.
[5]Institute of Geophysics and Planetary Physics, University of California, San Diego, La Jolla, California.
[6]Seismological Laboratory, University of Nevada at Reno, Reno, Nevada.

Paper number 2001JB000178.
0148-0227/01/2001JB000178$09.00

Those previous Moho depth estimates for the Peninsular Ranges were all made north of the international border. To achieve further understanding of the relationships among surface elevation, crustal thickness, and extension in this region, we determine crustal thickness across the Baja California peninsula, México, using receiver function estimates of teleseismic Moho *Ps* delays. Station placement for this study is near latitude ~31°N (Plate 1). This location is sufficiently near the profile of *Ichinose et al*. [1996] (the latter is just north of the international border) to permit informative comparisons yet south of the complications associated with extensive strike-slip faulting north of the Agua Blanca fault. The profile runs the full breadth of the Peninsular Ranges, traversing the highest elevation on the peninsula, the ~2.7-km-high Sierra San Pedro Mártir. It crosses the Main Gulf Escarpment at the Sierra San Pedro Mártir fault zone where the escarpment is especially well expressed topographically. The profile also includes several stations within the Gulf Extensional Province on the Baja peninsula, one station on the eastern (mainland) shore of the Gulf of California, and one station within the gulf itself.

In sections 2–4, we review the geologic setting for the study, describe the station deployment and data analysis, and present the first crustal thickness estimates obtained on the Baja California peninsula. In section 5 we compare the inferred Moho configuration with the related southern California studies and discuss their relationship to surface topography and gulf rifting. The geographical area under discussion straddles the international border to include portions of the state of California, United States, and the state of Baja California, México.

We use the designations "Alta California" and "Baja California," respectively, to distinguish the areas north and south of the international border.

2. Geologic Setting

Southern Alta California, United States, and the northern part of the peninsula of Baja California, México, comprise a geologically complex region that has experienced a major orogeny associated with Mesozoic arc magmatism overprinted by Cenozoic strike-slip and extensional faulting accompanying modern continental rifting to the east (Plate 1). The region can be divided into three structural domains: the Transpeninsular Strike-slip Province, the Gulf Extensional Province, and the Stable Central Peninsula [*Stock et al.*, 1991]. The Transpeninsular Strike-slip Province contains the dextral Elsinore fault, San Jacinto fault, and other strike-slip fault zones in southern Alta California and northern Baja California that comprise elements of the diffuse boundary between the Pacific and North American plates. The Agua Blanca fault forms the southern boundary of the Transpeninsular Strike-slip Province. This right-lateral fault may represent an accommodation zone that separates a reversal in vergence along the Main Gulf Escarpment, which marks the western edge of upper crustal gulf rifting [*Axen*, 1995].

The Gulf Extensional Province extends south from the Salton Trough in southern Alta California along the eastern side of the Baja California peninsula. The waters of the Gulf of California have intruded a structural depression created by detachment and oblique rifting of the peninsula from mainland México [*Lonsdale*, 1989]. Initiation of east-west directed extension during the middle Miocene (~17–9 Ma) may have weakened the crust in the vicinity of the gulf, facilitating propagation of the Pacific–North American plate boundary into the gulf in Pliocene time [e.g., *Dokka and Merriam*, 1982]. The plate boundary in northern Baja California and southern Alta California is presently manifested in a broad zone of distributed transtensional shear [*Lewis and Stock*, 1998].

The Main Gulf Escarpment separates the Gulf Extensional Province and the Stable Central Peninsula. Two major approximately north-south striking fault zones control the escarpment [*Axen*, 1995]: the Sierra San Pedro Mártir fault system to the south and the Cañon David detachment fault to the north (Plate 1). *Axen* [1995] suggested that the steep front of the Sierra Juárez is an antithetic faulted rollover structure that soles into the west directed Cañon David detachment. The steep front of the Sierra San Pedro Mártir is the footwall scarp to the breakaway faults of an east directed fault system [*Axen*, 1995]. The sinuous map trace and hanging wall geology of the 100-km-long Sierra San Pedro Mártir fault system suggest that it is probably listric [e.g., *Dokka and Merriam*, 1982]. Structural relationships of volcanic units at ~31°N latitude indicate that half of the 5 km of maximum normal displacement along the Sierra San Pedro Mártir fault occurred between 11 and 6 Ma [*Stock and Hodges*, 1990]. A number of Holocene normal fault scarps with as much as 25 m of vertical separation have been observed along the length of the Sierra San Pedro Mártir fault system [*Brown*, 1978], and the Boletín de la Red Sísmica del Noroeste de México (RESNOM) documents present-day microseismicity on the fault. These data indicate that the fault is presently a locus of extensional strain. To the south, the fault system becomes more discontinuous, and displacement as well as topographic relief on the faults decrease significantly.

The Stable Central Peninsula is west of the Gulf Extensional Province and south of the Agua Blanca fault and is composed largely of the Mesozoic Peninsular Ranges batholith. The batholith can be divided compositionally into western and eastern zones, which likely reflect different source regions [e.g., *Silver and Chappell*, 1988]. The older, more mafic western section formed in oceanic lithosphere; the younger, more silicic eastern section developed in continental lithosphere [*Silver et al.*, 1979; *Gastil*, 1993]. Juxtaposition of oceanic and continental lithosphere may have occurred during a Permo-Triassic event that truncated western North American continental lithosphere [e.g., *Burchfiel et al.*, 1992]. The boundary separating these two crustal domains, which we refer to as the compositional boundary, is defined by geophysical, geochemical, and petrological discontinuities along the entire length of the batholith [e.g., *Gastil et al.*, 1975]. *Thomson and Girty* [1994] suggested that the compositional boundary provided a mechanical weakness in the crust along which Mesozoic intra-arc strain was concentrated. *Magistrale and Sanders* [1995] proposed that Quaternary fault development in southern Alta California has also been localized at this discontinuity.

3. Data and Analysis

The North Baja Transect (NBT) stations, a collaborative effort by el Centro de Investigación Científica y de Educación Superior de Ensenada in México, San Diego State University, the Southern California Earthquake Center, the University of California, San Diego, and the University of Nevada at Reno, ran from October 1997 through June 1998 [*Astiz et al.*, 1998]. Nine of the 11 temporary three-component broadband stations used Guralp CMG40T seismometers, with response flat to velocity in the band ~0.03–16 Hz. Stations SAFE and PUPE (Plate 1) used Guralp CMG3ESP seismometers, with response flat to velocity in the ~0.01–16 Hz (SAFE) and ~0.03–16 Hz (PUPE) bands. Each station was equipped with a 24-bit digitizer recording at 40 samples per second. To investigate the relation between Moho depth and topography, the stations were positioned in northern Baja California, México, south of the Transpeninsular Strike-slip Province with ~15-km spacing along an approximate east-west transect at ~31°N (Plate 1). Six of the stations traversed the Stable Central Peninsula, where elevations range from nearly sea level at the Pacific coast to just under 3 km at the axis of the Peninsular Ranges. The other five stations were located east of the Sierra San Pedro Mártir fault in the Gulf Extensional Province, which included one station on the island of Roca Consag in the Gulf of California and one on the mainland México side of the Gulf at Puerto Peñasco. Most stations ran for about a 6-month period, with the exception of the island instrument, ROKO, which recorded for about a month before being disabled by sea lions. Despite the high noise level at this station, a few teleseismic events were recorded during its brief life span. Over the deployment period, the remaining stations recorded 15 large teleseismic events in the epicentral distance range $30° < \Delta < 100°$, 11 of which were $M_w > 6.5$, that were suitable for use in the analysis (Table 1).

3.1. Receiver Functions

We select records of teleseismic earthquakes with impulsive, high signal-to-noise P waves. The records are rotated to the great circle path, cut to 60-s cosine-tapered windows, and band-pass filtered (0.05–0.7 Hz). Receiver functions are determined through frequency domain deconvolution of the radial horizontal component by the vertical component, which isolates and enhances P-to-S converted phases [e.g., *Langston*, 1979; *Owens et al*., 1984; *Ammon et al*., 1990]. The spectral division is regularized by raising the amplitude spectrum of the vertical component to 1% of its RMS level whenever it would otherwise fall below this minimum (the so-called "water level" method of regularization). The deconvolved record is then low-passed with a zero-phase filter with two-pole Butterworth amplitude response and its corner at 0.7 Hz. The signal-to-noise ratio is increased by stacking the receiver functions within bins defined by epicentral distance and back azimuth. Five different back azimuth bins ranging from 10° to 320° are defined, wherein each bin contains a single event or several events covering up to 20° in back azimuth (see Table 1). Where multiple events from the same back azimuth bin are available, we consistently find a high degree of similarity in the individual event estimates of the receiver function, and therefore we have retained some single-event bins (e.g., the Greenland event in Table 1) in the analysis. Each stacked receiver function from a different back azimuth provides a point depth estimate. The Ps conversion occurs at a point which is offset horizontally (in the back azimuth direction) from the receiving station, the amount of offset depending upon ray parameter; we will refer to the surface projection of this point as the conversion projection point. Data from multiple back azimuths help to confirm the interpretation of Ps picks as Moho conversions and also may provide insight on lateral variation of Moho depth near the station. The transverse horizontal component potentially provides additional information on the attitude of the interface producing the converted phase [*Cassidy*, 1992]. Here we interpret only the radial receiver functions, but we use the transverse components to identify those traces for which the Moho Ps phase is likely to be complicated by laterally scattered phases. Station-source pairs with a transverse component receiver function amplitude exceeding that of the radial component are excluded from the analysis of crustal thickness.

3.2. Velocity Model

We use a flat-layered velocity model to convert each Ps-P time to Moho depth, allowing for different layer velocities beneath each station. Refraction studies constrain the regional average P wave velocity (V_p) along strike of the Peninsular Ranges [*Nava and Brune*, 1982], but the local crustal velocity variations have not been independently characterized at the latitude of the NBT stations. Since the regional peninsular geology varies minimally along structural strike, a correlative velocity model from southernmost Alta California, with modifications discussed below, was used to convert the Ps-P differential travel times to depth (Table 2). An east-west cross section is extracted from the three-dimensional southern Alta California crustal P wave tomographic results of *Magistrale* [1999] located at ~32°45′N in the approximate orientation of the transect of the NBT stations. This cross section is located just north of the international border, near the location of the *Ichinose et al*. [1996] station array shown in Plate 1. The compositional boundary coincides with a major crustal-scale velocity discontinuity [*Magistrale and Sanders*, 1995] and is used as an alignment reference when applying the Alta California velocity model to Baja California. For stations on the batholith we construct a one-dimensional depth-dependent P wave velocity model under each station by taking a velocity-depth profile from the southern Alta California cross section at the corresponding east-west position relative to the compositional boundary. In accordance with *Fuis et al*. [1982] and *Parsons and McCarthy* [1996] the deepest crustal velocities of the eastern Peninsular Ranges are capped at ~7.2 km/s to reflect the gabbro subbasement of the Salton Trough inferred from refraction and gravity.

For the five stations in the Gulf Extensional Province, we use the Salton Trough portion of *Magistrale*'s [1999] Alta California cross section but with station-specific modifications to the upper layer based on assumptions about the presence or absence of low-velocity sediments. At stations SAFE and PUPE, on the margins of the Gulf of California, we have included a 2-km-thick low-velocity (~2.6 km/s) surface sedimentary layer. Station SACA lies in the central Valle de San Felipe, which is a deep half graben filled with ~2.5 km of sediment [*Slyker*, 1970], and we extend the low-velocity layer to 2.5 km depth at SACA. We leave out the low-velocity sediment layer at ELAR, as it is located atop an outcrop of bedrock. We also leave out the sediment layer at ROKO, since *Allison* [1964] (citing from T. H. van Ande (personal communication)) describes Roca Consag as andesitic. The Moho depth estimates are not too sensitive to these assumed variations in the sediment layer. For example, a 1-km variation in thickness of the low-velocity (~2.6 km/s) layer adds ~1 km of variation to the depth estimates. In section 4 we examine the teleseismic P wave travel time residuals and find that they are consistent with the above assumptions for the sediment thicknesses.

We also need an S wave velocity (V_s) model at each station, which we construct from the V_p model assuming a constant velocity ratio V_P/V_S. The refraction results of *Nava and Brune* [1982] and the tomography results of *Scott* [1992] both suggest an average V_P/V_S ratio of 1.73 for the Peninsula Ranges in Alta California, and we adopt this value. As a rough indication of the uncertainty in V_P/V_S, we note that *Zhu and Kanamori* [2000] used teleseismic converted phases and their multiple reflections to estimate a somewhat higher average V_P/V_S of 1.78 for the southern Alta California crust.

A Moho depth estimate is obtained for each receiver function stack by varying the thickness of the lowermost crustal layer in the velocity model to fit the observed Ps-P time. The Ps-P time calculation takes into account station elevation and the ray parameter specific to each receiver function. We give each Moho depth relative to sea level and associate the depth with the geographical location corresponding to the conversion projection point. This procedure yields several depth points for each station, one for each back azimuth bin for which a receiver function is obtained.

3.3. Travel Time Residuals

Our estimates of crustal thickness rely principally on the timing of converted phases identified in receiver functions. However, we also examine the travel times of the direct P waves, as these provide a rough cross-check on our assumed velocity model. For this purpose, we model the P wave residuals, relative to the IASPEI tables [*Kennett and Engdahl*, 1991], as the sum of an event term and a station term. That is, the residual for event i at station j, ΔT_{ij}, is modeled as

$$\Delta T_{ij} = E_i + S_j + \varepsilon_{ij}, \tag{1}$$

in which E_i, $i = 1, \ldots, N_E$ (where N_E is the number of events) are the event delay terms, S_j, $j = 1, \ldots, N_S$ (where N_S is the number of stations) are the station delay terms, and ε_{ij} are random errors. Variations in the station terms should

Table 1. Locations and Magnitudes of Events Used in Teleseismic Receiver Function Analysis at North Baja Transect Stations[a]

Event	Origin Time, UTC	Latitude, deg	Longitude, deg	~Δ, deg	~BAZ, deg	Depth, km	M_w	Stations[b]
			Greenland					
1998080	163311.00	79.82	1.24	64	10	10	6.2	a, b, g, h, k
Andes								
1998010	045425.39	−11.89	−71.99	60	128	33	6.4	a, b, d, f, g
1998012a	101407.63	−31.03	−71.38	75	141	34	6.6	a, b, e, f
1998030	121608.69	−23.69	−70.01	70	135	42	7.1	a, d, e, f, h, k
1998050	042130.53	−10.87	−74.34	58	129	33	6.0	k
1998091	224256.90	−40.36	−75.19	80	150	9	6.7	h, k
1998142	044850.44	−17.55	−65.14	67	129	24	6.6M_s	k
			South Pacific					
1998004	061158.97	−22.20	171.06	88	242	100	7.5	a, b, d, g
1998012b	163620.23	−15.93	−179.33	77	242	23	6.9	a, b, e, f, i
1998171	202445.17	−30.01	−177.69	86	231	57	6.0	k
			North Pacific					
1998001	061122.64	23.93	141.93	87	297	95	6.6m_b	a, b, e, f, i, k
			Aleutian					
1997339a	112654.69	54.85	161.99	61	319	33	7.8	b, e, f, h, j
1997339b	184822.79	53.87	161.48	61	318	33	6.6	b, e, f, h, j
1997351	043851.46	51.20	178.87	52	313	20	6.6	a, b, c, d, e, f, h
1998152	053403.58	53.00	159.99	63	318	43	6.9	k

[a]Here ~Δ is approximate epicentral distance, and ~BAZ is approximate back azimuth.
[b]Stations that used event in receiver function analysis: a, TELM; b, LOQI; c, LACB; d, SAJO; e, ALAM; f, OBTO; g, SACA; h, ELAR; i, SAFE; j, ROKO; k, PUPE.

reflect crustal velocity variations beneath the stations (plus effects of Moho topography and upper mantle velocity variations). The estimation of the $N_E + N_S$ unknown parameters is complicated by missing data (each event is recorded at only a subset of the stations) and the prevalence of outliers in the arrival time data.

We estimate the station and event terms by the following procedure. First, we correct each travel time for station elevation, so that ΔT_{ij} is the travel time residual reduced to sea level. We then minimize the sum of misfit absolute values, F, given by

$$F = \sum_{ij} |E_i + S_j - \Delta T_{ij}|, \tag{2}$$

where the sum is taken over all event-station pairs for which there are data. There are, of course, standard algorithms for solving an L_1 optimization problem like (2), but an extremely simple iterative scheme suffices in this special case. Note that if all the E_i values were known, F would be minimized by setting each S_j to the median value of $\Delta T_{ij} - E_i$ (with j held fixed). Likewise, if all the S_j values were known, F would be minimized by setting E_i to the median of $\Delta T_{ij} - S_j$ (with i held fixed). Therefore the minimization problem is solved by a fixed point of the iteration

$$S_j^{(k)} = \text{median } (\Delta T_{ij} - E_i^{(k-1)}), \ j = 1, \ldots N_S \tag{3a}$$

$$E_i^{(k)} = \text{median } (\Delta T_{ij} - S_j^{(k)}), \ i = 1, \ldots N_E. \tag{3b}$$

which, after initialization by $E_i^{(0)} = \text{median}(\Delta T_{ij})$, converges quickly. We then repeat the solution of (3) after removal of data points with misfit exceeding 3 times the RMS misfit. Finally, we compute the standard error estimates for the station delays by the jackknife method [*Efron*, 1982], i.e., resampling with one data point excluded from each sample. Station ROKO was not included in the travel time analysis, as it recorded too few events to yield a meaningful station delay estimate.

Table 2. Crustal P Wave Velocities as a Function of Depth Used at Each North Baja Transect Station to Estimate Depth to Moho[a]

	Station										
Depth, km	TELM	LOQI	LACB	SAJO	ALAM	OBTO	SACA	ELAR	SAFE	ROKO	PUPE
0–2	5.13	5.22	5.14	5.03	4.97	4.77	2.50[b]	4.94	2.63	4.33	2.63
2–4	5.36	5.54	5.42	5.29	5.26	5.07	5.02	4.96	4.33	4.33	4.33
4–8	6.24	6.82	6.42	6.74	5.97	6.21	5.88	6.07	5.68	5.68	5.68
8–12	6.63	6.51	6.82	6.45	6.19	6.24	6.02	6.17	6.38	6.38	6.38
12–17	6.62	6.44	6.74	6.68	6.20	5.96	6.22	6.47	7.07	7.07	7.07
17–22	6.74	6.69	6.60	6.94	6.73	6.41	7.21	7.21	7.21	NA	NA
>22	6.79	6.79	6.79	6.79	6.79	6.79	7.21	7.21	NA	NA	NA

[a]Velocities are in km/s. Velocity structure is based on that of *Magistrale* [1999] southern Alta California 3-D P wave tomography. Construction of the velocity model is discussed in text. NA, not available.
[b]The 2.50 km/s sediment velocity is applied to depth 0–2.5 km, 5.02 km/s velocity is applied to depth 2.5–4 km at SACA.

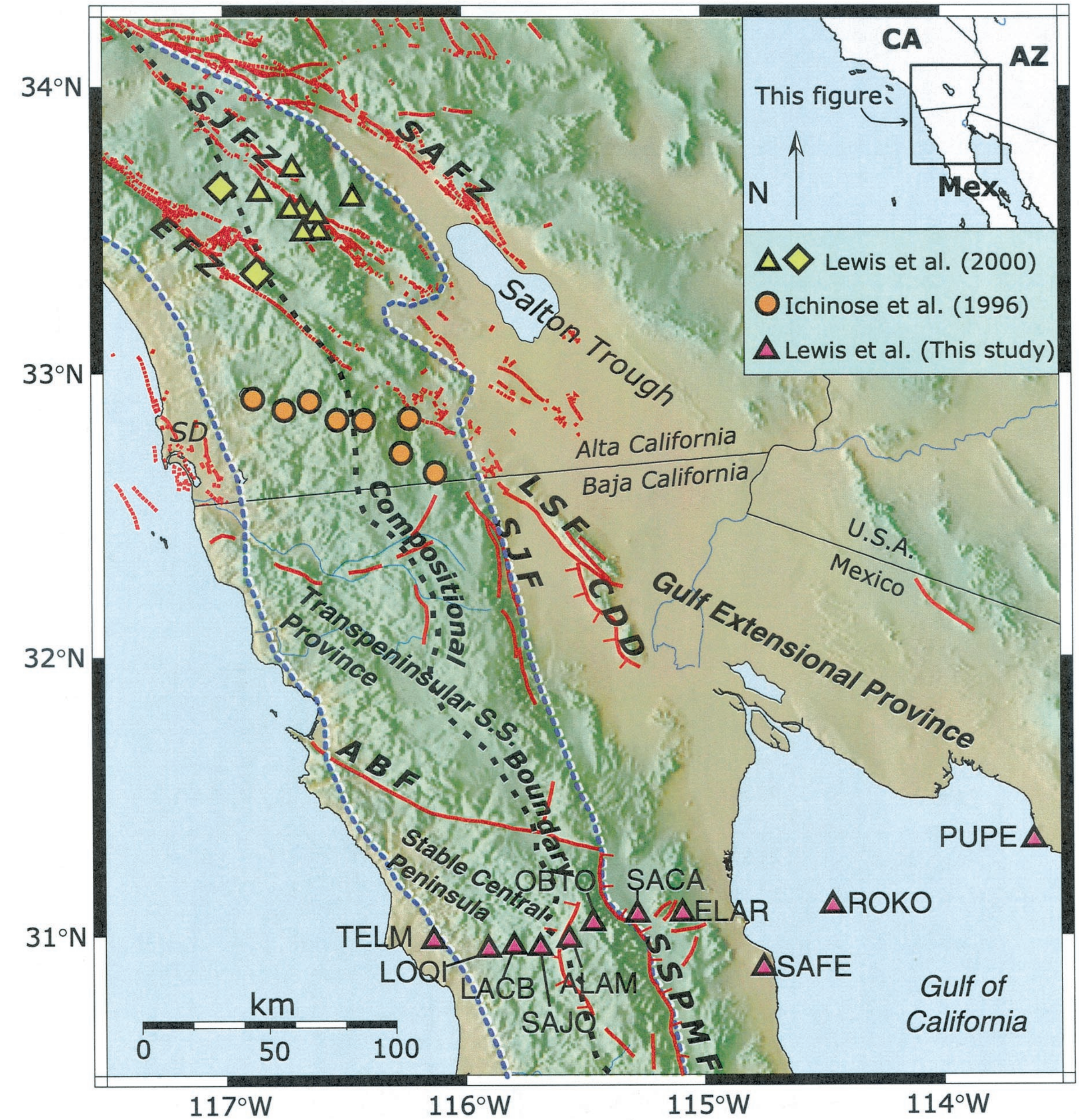

Plate 1. Map of Peninsular Ranges (outlined with dashed blue lines) and Gulf Extensional Province with topography. The Transpeninsular Strike-slip Province and Stable Central Peninsula are Peninsular Ranges structural domains lying north and south, respectively, of Agua Blanca fault (ABF). Yellow diamonds/triangles and orange circles represent stations used in related studies by *Lewis et al.* [2000] and *Ichinose et al.* [1996], respectively. Red triangles (labeled) represent stations of North Baja Transect. Black dashed line is compositional boundary; red lines are faults. Abbreviations are ABF, Agua Blanca fault; CDD, Canon David detachment; EFZ, Elsinore fault zone; LSF, Laguna Salada fault; SD, San Diego; SJF, Sierra Juarez fault; SJFZ, San Jacinto fault zone; SAFZ, San Andreas fault zone; SSPMF, Sierra San Pedro Mártir fault.

3.4. Uncertainty Considerations

Southward projection of the *Magistrale* [1999] southern Alta California tomographic model introduces uncertainty in V_P. To gauge this uncertainty, we compare two east-west Peninsular Ranges cross sections separated by ~80 km in latitude within the study area of *Magistrale* [1999]. Only the total vertical travel time affects the Moho depth estimate. The single-layer vertically averaged velocity that yields the same total vertical travel time as the layered model is given by $(\Sigma h_i)/\Sigma(h_i/V_{Pi})$, where the ith layer has thickness h_i and P wave velocity V_{Pi}. Vertically averaged P wave velocities contrast by <2% at corresponding positions along the two cross sections, so we conclude that the east-west V_P profile of the Peninsular Ranges varies little along structural strike. Within the Peninsular Ranges, then, velocity variability between latitudes plays a small role in uncertainty estimates. In the Gulf Extensional Province, uncertainty in thickness and velocity of the surficial sediments leads to uncertainty in vertical P wave travel time which we estimate at ~0.15 s, which contributes ~5% to Moho depth uncertainty.

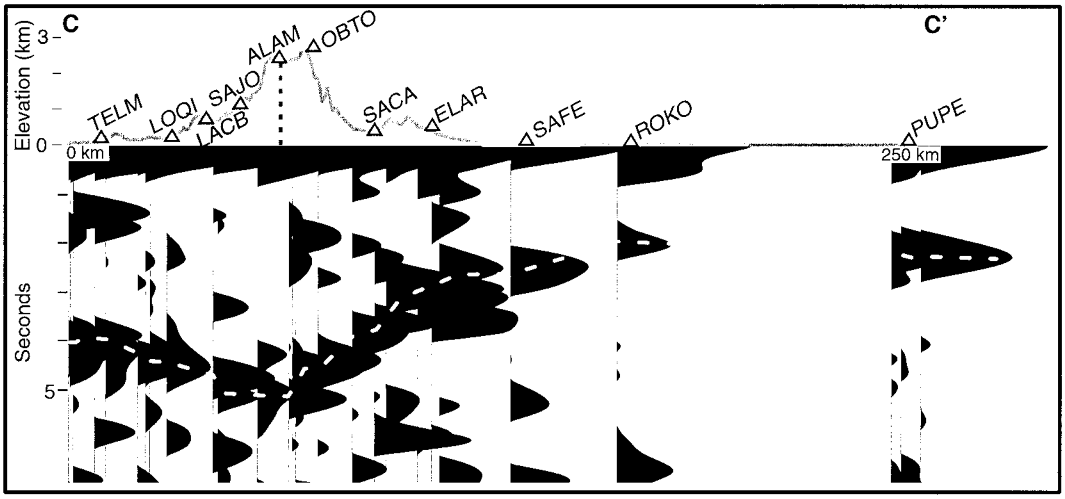

Figure 1. Record section of receiver function peaks calculated at North Baja Transect stations (triangles) plotted with topography. Receiver functions have not been corrected for surface topography, or for move out due to variations in ray parameter. Dashed white line indicates arrival interpreted as Moho *Ps* conversion. For clarity, negative values of receiver functions are not shown. Dashed vertical line represents compositional boundary. Cross section location is shown in Figure 3.

Since *Ps*-*P* travel time represents the differential travel time of *S* relative to *P*, errors in V_P/V_S introduce another source of uncertainty [*Zhu and Kanamori*, 2000]. The regional V_P/V_S ratio estimates from refraction [*Nava and Brune*, 1982], tomography [*Scott*, 1992], and teleseismic converted phase analysis [*Zhu and Kanamori*, 2000] vary by ~3%, contributing ~7% uncertainty in crustal thickness.

Another source of uncertainty in Moho depth results from assuming that the *P*-to-*S* conversion occurs at a locally horizontal interface. For the ~25° local dip found beneath the NBT in the eastern Peninsular Ranges, this uncertainty is, for instance, ~2 km for a 30-km-thick crust, or ~6%. While the influence of a nonhorizontal Moho on the depth estimate is relatively minor, lateral shifts of the conversion projection point can be somewhat greater. Relative to a flat crust-mantle interface, a Moho with a 25° dip shifts the conversion projection point ~10 km in the updip direction. For a ~10° dipping Moho (as found beneath the western peninsula), updip shift of the conversion point is negligible. The general configuration of the Moho is little affected by the shifts of the conversion projection points due to Moho dip, which we will specifically discuss in section 5.

In most cases, our estimate of the error in picking the *Ps* arrival time is <0.1 s (the few exceptions, noted below, occur when interfering arrivals result in ambiguity in identification of the *Ps* phase), contributing ~2–4% variation in the Moho depth estimate. Treating the above sources of error (V_p, V_p/V_s ratio, interface dip, and time picks) as independent, random contributions to error, we estimate a standard error of ~11% for the Moho depth estimates.

4. Results

Receiver functions are obtained at each station for one or more of the five back azimuth bins. They generally exhibit a strong, spatially coherent arrival within the first 5.25 s. The relative strength and spatial coherence of this phase are most evident when the receiver functions are arranged in the form of a record section, as in Figure 1. In Figure 1 the geographic location of each receiver function trace has been projected onto an approximately east-west cross section. For this purpose, the trace was assigned a geographical location corresponding to a *Ps* conversion point at a 30-km-deep interface, as computed from the appropriate ray parameter and back azimuth. The phases which we have identified as the Moho *Ps* conversion have been indicated in Figure 1 by a dashed white curve (e.g., at ~4 s at station TELM). In Figure 1 we have not yet corrected for elevation, velocity, and ray parameter variations, but Figure 1 nonetheless provides a reasonable qualitative view of the Moho geometry. Figure 2 shows the receiver function traces in more detail, and Figure 3 shows the location of the cross section and the inferred Moho depths after all corrections have been made.

The identification of the Moho *Ps* is in most cases relatively unambiguous, as can be seen from the simplicity of the indicated phases in Figure 2. The most notable exceptions are the double peaks for the Aleutian and Andes traces at LOQI and the Aleutian trace at ALAM. The initial, direct *P* wave pulse is also very simple at most stations. Some broadening of the direct *P* pulse is evident at SACA (especially the Andes trace), ELAR (Greenland and Aleutian traces), and ROKO, a feature that typically results from interference of the direct *P* wave with converted phases generated within a few kilometers of the station, for example, at the base of a sedimentary layer. In the present case, the broadening does not appear to have a simple interpretation in the context of flat-layered structure, as it is not consistent for different source azimuths recorded at a given station, nor does its occurrence show a consistent relationship to surface geology (e.g., pulse broadening is observed for some sources recorded at SACA, which overlies a deep sedimentary layer, but also at ELAR, which is sited on bedrock). A tendency is also suggested by Figure 2 for the Moho *Ps* amplitude to be higher (relative to direct P) at the five stations in the Gulf Extensional Province (SACA, ELAR, SAFE, ROKO, PUPE)

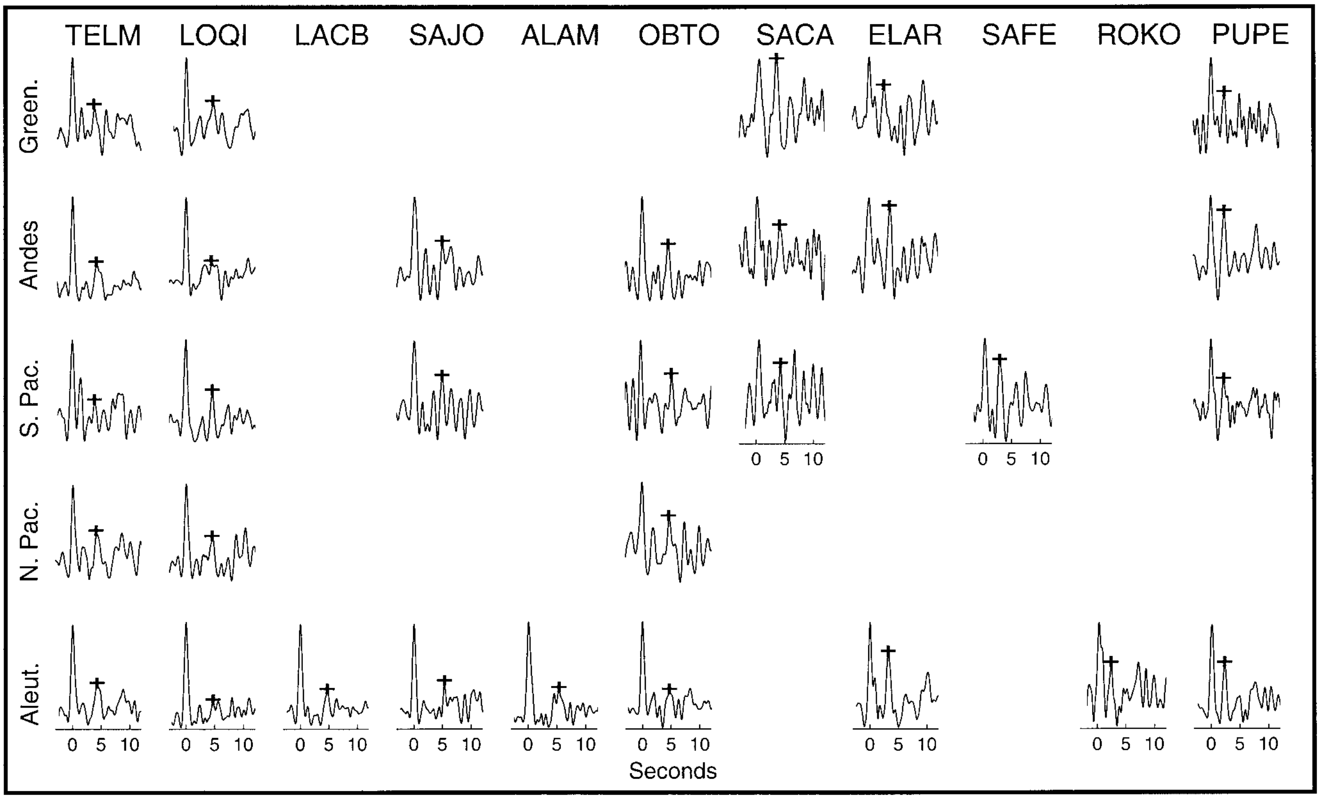

Figure 2. Radial receiver functions determined at each North Baja Transect station (columns are stations displayed in west to east order) for each source region (rows) ordered by back azimuth. Direct *P* arrivals are peaks at zero time. Arrivals interpreted as *Ps* are indicated by crosses. Abbreviations are Green., Greenland; S. Pac., South Pacific; N. Pac., North Pacific; Aleut., Aleutians.

than at the six Peninsular Ranges stations. If real, this difference between provinces could be indicative of a change in the physical nature of the Moho (e.g., the velocity contrast across the Moho).

Figure 3 summarizes the results of the Moho depth calculations. Depth below sea level to the Moho in the northern Baja California peninsula varies smoothly from ~33 (±3) km near the Pacific coast to ~40 (±4) km just west of the compositional boundary, then shallows abruptly, reaching ~15 (±2) km in the center of the Gulf of California. Moho depth appears relatively constant across the width of the gulf, although measurements are sparse there, and depths beneath the mainland Mexican Gulf Coast suggest a slight eastward thickening of the crust. While Moho topography varies gradually with surface elevation in the western Peninsular Ranges, a steep apparent Moho dip of >20°W is found beneath the

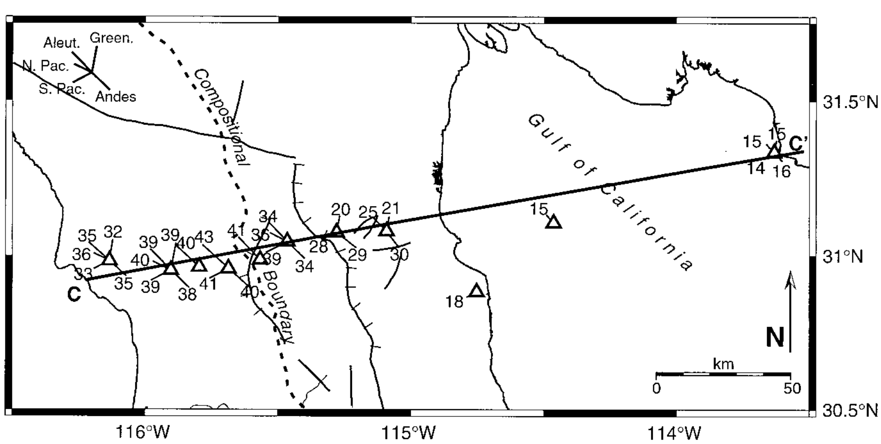

Figure 3. Map of North Baja Transect stations (triangles) and corresponding Moho depths, relative to sea level, plotted at conversion projection points from different back azimuths. The depth determinations include adjustments for station elevations as well as for the ray parameter appropriate to each source region. Dashed line is compositional boundary; other lines are faults and shorelines. Source region abbreviations are Green., Greenland; S. Pac., South Pacific; N. Pac., North Pacific; Aleut., Aleutians.

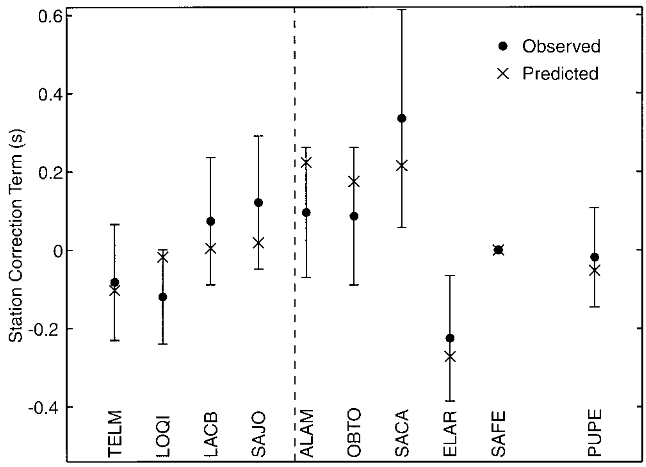

Figure 4. Teleseismic *P* wave station delays relative to station SAFE, with their standard errors, at North Baja Transect stations. Also shown are predicted delays based on velocity model given in Table 2 with crustal thicknesses shown in Figure 3. ROKO recorded too few events to be included in the analysis. Dashed vertical line represents approximate location of compositional boundary.

eastern Peninsular Ranges. The deepest Moho is offset westward from the highest surface elevation by ~20 km. Moho depth directly beneath the surface high is ~5 km shallower than the maximum Moho depth of ~40 km.

The back azimuthal variations of the *Ps-P* times for the majority of the stations are minimal and systematic over the aperture of a single station. However, large variations in *P-Ps* times with back azimuth are found at stations SACA and ELAR, with smaller differential travel times toward the north in both cases. These stations were positioned in the low Valle de San Felipe east of the steep Main Gulf Escarpment and just south of an accommodation zone [*Axen*, 1995]. In this tectonically complex location the variability of *Ps-P* time may be due to side scatterers interfering with the *Ps* arrival in this passband rather than the presence of radical changes in local Moho topography. Some of the *Ps* amplitudes are also unusually large at these two stations, approaching or exceeding the direct *P* wave amplitude in some instances, which might be indicative of the presence of multiple, interfering arrivals. However, we cannot exclude the alternative interpretation that the time variations represent actual complexity in the Moho. The Moho depth estimates obtained by averaging *Ps-P* times over all available back azimuths at stations SACA and ELAR are ~26 and ~25 km, respectively. These values fall between the average values of the station to the west, OBTO (~35 km), and the station to the east, SAFE (~18 km). Despite the large back azimuthal variations in *P-Ps* times at SACA and ELAR, the overall pattern of a sharp eastward shallowing of the Moho beneath the eastern peninsula is evident.

Figure 4 shows the station delay terms, relative to station SAFE, as estimated from the analysis of 125 elevation-corrected travel time residuals. Station ROKO recorded too few arrivals to be included in the travel time analysis. For comparison, predicted station delays are also shown in Figure 4. The latter are calculated using the crustal velocity models in Table 2, combined with the average Moho depth at each station as estimated from the receiver functions, and assuming an uppermost mantle velocity of 8 km/s. The calculation of predicted station delays was done for a ray slowness of 0.06 s/km, which represents the mean of the observations used. The predicted delays are within a standard error of the station term estimate. This agreement provides a useful cross-check, confirming that our velocity model and inferred Moho configuration are consistent with the travel time data. The standard errors are too large to provide an independent validation of velocity model details, but the precision is sufficient to confirm the presence of the deep, low-velocity sediment layers beneath SACA, SAFE, and PUPE and its absence beneath ELAR. For example, nearly all (~0.5 s) of the predicted difference in *P* wave delay between SACA and ELAR is due to the low-velocity sediment layer in our SACA model, and this difference agrees well with the observed difference in station delays of 0.6 ± 0.2 (the uncertainty estimate for the SACA-ELAR difference has taken into account a positive covariance which we find between the SACA and ELAR estimates).

The predicted delays in Figure 4 neglect possible additional delays due to velocity anomalies in the mantle, e.g., reduced upper mantle velocity beneath the Gulf Extensional Province. In that case, we would be overestimating the sediment delays. However, mantle effects are likely to be smaller than the measurement errors in the station residuals. For example, a 3% velocity anomaly over 50 km depth in the mantle would produce only ~0.15 s of *P* wave travel time delay, which would not substantially alter our conclusions about the presence of sediment delays.

5. Discussion

The Moho attains its maximum depth, ~40 (±4) km, to the west of both the compositional boundary and the maximum surface elevation. From this maximum depth the Moho shallows gradually (~10° dip) toward the west. It also shallows very abruptly to the east of its depth maximum, dipping ~25° under the topographically high Sierra San Pedro Mártir and reaching ~18 (±2) km depth at the western edge of the Gulf of California. We compare these results, the first crustal thickness profile obtained on the Baja California peninsula, with recent, related studies from north of the international border to obtain a consistent regional pattern of Moho variations in the Peninsula Ranges and Gulf Extensional Province of southern Alta California and northern Baja California.

5.1. Peninsular Ranges Moho Depth

Both *Ichinose et al.* [1996] and *Lewis et al.* [2000] obtained Moho depth profiles across the southern Alta California Peninsula Ranges and found the deepest Moho under the western part of the batholith. Those profiles are compared with the Baja California profile in Figure 5. At ~33°45′N latitude (cross section A-A′ in Figure 5) the maximum Moho depth, ~37 km, occurs under the western Peninsular Ranges, shallowing (with a ~10° dip) under the high elevations of the eastern Peninsular Ranges [*Lewis et al.*, 2000]. At ~33°N (cross section B-B′ in Figure 5), Moho depths are again maximum (36–41 km) in the western Peninsular Ranges, shallowing even more steeply (~20°) beneath the eastern Peninsular Ranges [*Ichinose et al.*, 1996]. The current northern Baja results at ~31°N (cross section C-C′ in Figure 5) continue this pattern of ~40 km depths under the western part of the range and abrupt shallowing under the topographic highs in the eastern part of the range. The Moho dips under the eastern part of the range are steeper on the two southern profiles (Figure 5) than on the northern

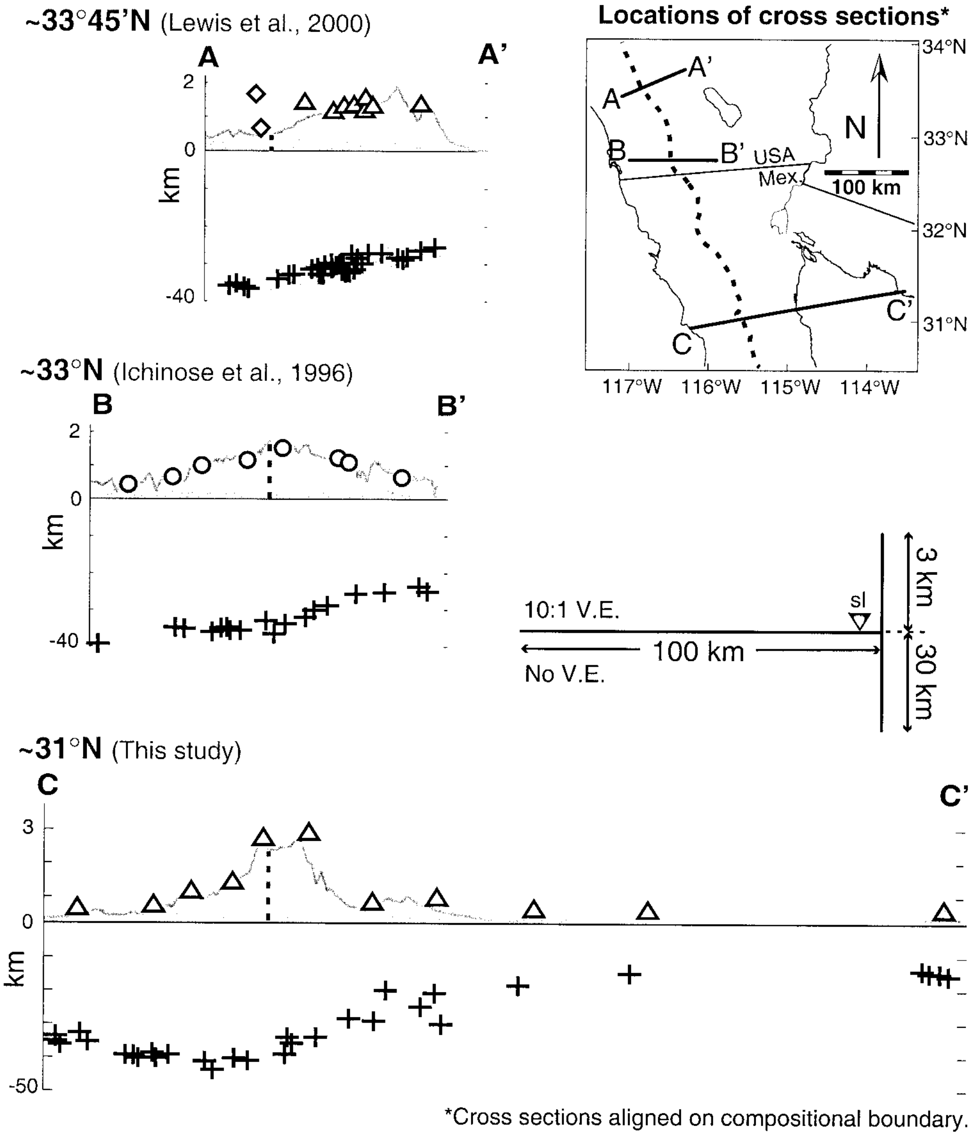

Figure 5. Cross sections of elevation and Moho depth along three latitudes of the northern Peninsular Ranges (locations shown on map). Cross sections are aligned on the compositional boundary, denoted by dashed vertical line. The crust thins dramatically beneath the eastern Peninsular Ranges, and the Moho shape does not reflect surface topography. Note the vertical exaggeration of the surface elevation.

profile. Taken together, these results support the suggestions of *Lewis et al.* [2000] that thinned crust is present regionally under the eastern Peninsular Ranges, that the crustal thinning represents a lower crustal response to Salton Trough/Gulf of California extension, and that steeper dips are associated with more mature portions of the rift margin.

The change in Moho attitude in these profiles occurs near the downdip projection of the compositional boundary (although this is less clear for the northernmost profile, since there are few data to the west). The apparent association may simply be fortuitous. We speculate that the compositional boundary limits the westward extent of rift-related crustal thinning, either because of partial mechanical decoupling at the boundary or because of differences in crustal rheology across the boundary. With respect to possible mechanical decoupling, there is evidence that the compositional boundary has served as a locus of mechanical weakness in the past [*Thomson and Girty*, 1994; *Magistrale and Sanders*, 1995]. With respect to rheological contrast, rocks of the eastern batholith are more silicic than those of the western batholith, and the seismic tomography of *Magistrale* [1999] suggests that the lithologic difference continues through the whole thickness of the crust. This lithological difference would be consistent with a somewhat lower creep strength for the eastern part of the Peninsular Ranges.

Off the west coast of Alta California, Moho depths near Santa Catalina Island in the continental borderlands are estimated at ~19–23 km from seismic and gravity data [*ten Brink et al.*, 2000] and at 21–22 km from teleseismic receiver functions [*Zhu and Kanamori*, 2000]. Although corresponding estimates are not available off the Baja California west coast, the onshore results are at least consistent with a transition to thinner crust offshore of Baja. The current study shows that Moho under the west coast of northern Baja is ~33 km deep, ~7 km shallower than the maximum depth, which occurs ~50 km inland.

5.2. Northern Gulf of California Moho Depth

East of the northern Peninsular Ranges, beneath the central Salton Trough in southern Alta California, which is the northern extension of the Gulf Extensional Province, the Moho depth has been estimated at 21–22 km from seismic refraction [*Parsons and McCarthy*, 1996]. Along the northern Baja California profile, ~200 km to the south, we obtain somewhat thinner crustal thickness estimates for the gulf province, ~18 km at the western margin of the gulf (at San Felipe, SAFE) and ~15–16 km within the northern gulf and on the eastern margin (at Puerto Peñasco, PUPE).

Our Moho depth range for the northern gulf, 15–18 (±2) km, is significantly shallower than the single previously reported northern Gulf Moho depth estimate from the marine refraction work of *Phillips* [1964], who inferred a depth "no less than 24 km." Phillips cites some serious observational and interpretational problems associated with the latter estimate, however. The refraction estimate was based on minimal observations (only 4 of the 16 profiles in the northern gulf show arrivals with high enough apparent velocity to be interpreted as Moho refractions), none of the profiles is reversed, and simple alternative interpretations are available for the few high apparent velocity events.

Our northern Gulf of California estimate of ~15–18 km indicates that the crust comprising the northern gulf is even thinner than that of the Salton Trough. The depths to the Moho on either side of the 125-km-wide northern gulf do not fluctuate greatly from the center estimate (18 km on the west coast and 15–16 km on the east coast), although the current sparse receiver function observations cannot rule out more localized crustal thickness variations between stations. Correlation of geologic units across the northern gulf [*Oskin and Stock*, 1999] indicates that post late Miocene upper crustal deformation has been localized. Heat flow in the Salton Trough and northern gulf is typically high (≥150 and >100 mW/m^2, respectively), but the data of the northern gulf do not show clearly localized areas of high heat flow [*Lachenbruch et al.*, 1985; *Henyey and Bischoff*, 1973; *Sanchez-Zamora et al.*, 1991]. The minimal variation in crustal thickness observed at the three stations in and on the margins of the northern gulf, in conjunction with the heat flow data and interpretations, suggest that the Salton Trough and northern gulf may embody a zone of diffuse lower crustal extension.

5.3. Isostatic Considerations

In each of the profiles of Figure 5 the maximum Moho depth is offset to the west of the maximum surface elevation. In each, the highest surface elevation occurs in the eastern Peninsular Ranges, above a steeply dipping Moho making a transition from depths of roughly 40 km in the western Peninsular Ranges to ~15–20 km depths under the Gulf Extensional Province. This pattern departs significantly from a simplified Airy model of local isostatic balance. That is, compensation of the high topography of the eastern Peninsular Ranges is not achieved through local crustal thickness fluctuations correlated to the surface topography. Nor is it likely that density variations confined to the crust can supply the additional buoyancy variations. For example, a strictly local compensation model for the Peninsular Ranges part of the NBT, with density variations confined to the crust, would require lateral variations in vertically averaged crustal density exceeding 6% between the site of the topographic high (~2.7-km-high Sierra San Pedro Mártir, with Moho depth ~35 km) and the site of the Moho depth maximum (~1 km elevations underlain by Moho depth ~40 km). This amount of lateral density variation appears unlikely, judging from the much smaller fractional variations in vertically averaged seismic *P* wave velocity (~3%) found in the geologically similar southern Alta California part of the range [*Magistrale and Sanders*, 1995]. It is therefore likely that compensation is achieved through local upper mantle density variations, flexural support, or both.

The elevation difference can be supported by plausible lateral variations in the upper mantle density alone. For example, if the upper mantle beneath the topographic high is assumed to have reduced density (relative to that beneath the western Peninsular Ranges) down to a total depth of 100 km (i.e., 65 km sub-Moho depth), then local support would require a density reduction of ~100 kg/m^3 (3%). If part of the required support is supplied by lateral density variations in the crust, then the magnitude of the required mantle density anomaly, its depth extent, or both, may be reduced.

If the lithosphere retains some elastic strength across the Peninsular Ranges–Gulf province transition (despite the large extensional strains and elevated temperatures), then the buoyancy source supporting the Peninsular Ranges topographic high need not be directly beneath that topographic high. Plausibly, support could come from forces transmitted laterally from the Gulf province to the Peninsular Ranges, via lithospheric flexure. Extension in the Gulf province entails a negative (i.e., upward) load upon the lithosphere (through mass removal via upper crustal brittle faulting and lower crustal ductile flow as discussed by *Egan* [1992], as well as from enhanced upper mantle buoyancy). Given some flexural rigidity of the lithosphere, part of that extension-related loading in the Gulf province may be transmitted westward to help support the Peninsular Ranges topographic high. For example, *Egan* [1992] used a two-dimensional (2-D) thin elastic plate model with an effective elastic thickness of 5 km to predict the flexural response of the lithosphere to 10–50 km of extension accommodated by a listric normal fault. The flexural response induces footwall uplift producing topographic relief of ~1.5 km at the rift edge, with the Moho uplifted by a similar amount beneath the topographic high. The quantitative results are sensitive to a number of model assumptions and parameters, including the total amount of extension. However, the postextension configuration of the (initially flat) Moho in Egan's computations has a consistent qualitative similarity to that observed along the NBT profile, with a topographic high at the rift margin offset from the maximum Moho depth.

Rather than repeat that modeling with parameters specific to the NBT profile, we perform a simplified calculation that does not address the origin of the topography and extensional loading (see Appendix A). We limit ourselves to showing that the inferred Moho shape is compatible with the present topographic load of the Sierra San Pedro Mártir, without the supporting buoyancy source necessarily being localized directly beneath the topographic high. Only a modest amount of lithospheric strength, equivalent to an effective elastic thickness of the order of 5 km, is required. Using a 2-D thin plate representation of the lithosphere [e.g., *Turcotte and Schubert*, 1982, pp. 122–123], we determine the amount of deflection of an initially flat, 34-km-deep Moho that is required to balance the loads imposed by the present topography plus a uniform upward load applied everywhere east of the Main Gulf Escarpment. The latter force schematically represents net unloading by brittle and ductile extension as well as any rift-induced

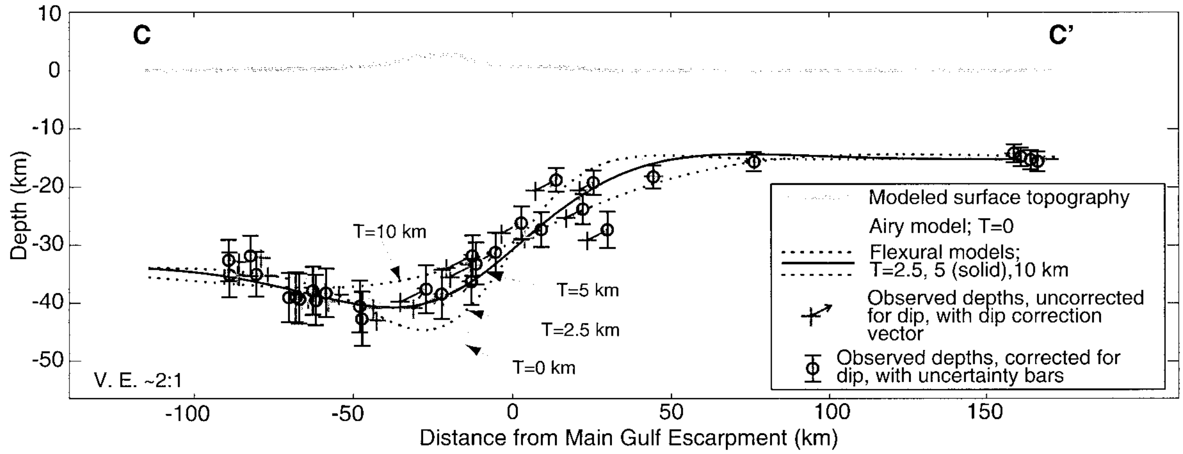

Figure 6. Observed dip-corrected Moho depths beneath North Baja Transect stations (circles with uncertainty bars) coincide, within error, with modeled Moho depths due to crustal flexure (solid and dotted curves). Crosses represent observed Moho depths assuming locally horizontal interfaces. While the Moho dip correction shifts the location of the *Ps* converted phase updip, the overall shape of the Moho is not altered significantly. This simple flexural model demonstrates that a modest amount of crustal strength, equivalent to an apparent elastic thickness *T* of the order of 5 km, can support the surface topography. Cross section location is the same as in Figure 3.

thermal sources of buoyancy. This negative force is scaled such that it flexes the Moho up to its observed depth of 15 km at large distances (relative to the flexural wavelength) east of the escarpment. A constant density contrast $\Delta\rho$ of 500 kg/m^3 is assumed at the Moho. The elastic and buoyant forces resulting from the deflection of the lithosphere are assumed to be in balance with the applied topographic and buoyancy forces.

Results of this simplified calculation are shown in Figure 6 for several values of the effective elastic thickness T. The calculation with $T = 0$ is equivalent to local Airy isostasy, in which case a ~50-km-deep Moho directly beneath the highest surface elevation would be required, contrary to observations. However, given a minimal amount of rigidity in the lithosphere, Moho deflection in this simplified model is compatible with the observed depth variations, including the lateral offset between the deepest Moho and maximum surface topography. An effective elastic plate thickness of the order of 5 km is required, which is comparable to the estimate of ~5 km for the northern Basin and Range [*Bechtel et al*., 1990]. Figure 6 also shows that correcting for shifts in the *Ps* conversion points due to ~25° Moho dip under Sierra San Pedro Mártir does not significantly affect the overall shape of the inferred Moho.

The thin plate calculation has substantial limitations. It neglects lateral changes in flexural rigidity and density. The modeled shape of the Moho reflects the vertical deflection of an initially flat Moho. The calculation does not directly account for weakening and thinning of the crust due to rifting nor the possibility of faults penetrating the entire thickness of the crust. Because of these and other simplifications the calculation probably somewhat overestimates the actual amount of flexure, and the inferred elastic thickness should be considered at best a rough estimate.

Lewis et al. [2000] noted seismic studies that illustrate the lack of an Airy root beneath the southern Sierra Nevada [*Jones et al*., 1994; *Fliedner et al*., 1996; *Wernicke et al*., 1996; *Jones and Phinney*, 1998], which is also a Mesozoic batholith. *Jones et al*. [1994] proposed that the high elevations of the Sierras are supported by mantle lithosphere that has been thinned and warmed in response to adjacent Cenozoic Basin and Range extension. As with the Sierras, the eastern Peninsular Ranges border an extensional terrane and may also be partially supported by local upper mantle heterogeneities. As we showed above, the vertical extent and magnitude of the required density anomaly appear to be geologically reasonable. We have also shown that it is possible that support for the high elevations in the eastern Peninsular Ranges is supplied partly or wholly by loads confined to the Gulf province and transmitted laterally into the eastern Peninsular Ranges by flexural rigidity of the lithosphere. The above calculation shows that only minimal effective elastic thickness would be required to make such a model viable.

6. Conclusions

Depth to the Moho beneath northern Baja California varies ~33 (±3) km near the Pacific coast, thickens gradually toward the east to ~40 (±4) km beneath the western Peninsular Ranges, then abruptly thins to ~15–18 (±2) km beneath the center and margins of the Gulf of California. The shallowing beneath the eastern Peninsular Ranges represents an average apparent westward dip of ~25°. These results corroborate the studies of *Ichinose et al*. [1996] and *Lewis et al*. [2000]. Together these studies all show that the Moho dip beneath the eastern Peninsular Ranges increases from ~10° near the northern extreme of the Salton Trough to >20° along the more mature portions of the rift margin.

Heat flow data and the presence of thin crust over a relatively large area in the Gulf Extensional Province suggest that the northern gulf and Salton Trough comprise a zone of diffuse lower crustal extension. Moreover, the region of extension may permeate the lower crust of the eastern Peninsular Ranges, tens of kilometers west of the zone of extensional deformation observed at the surface. Thinned crust underlies the topographic highs along 300 km of the eastern portion of the Peninsular Ranges, indicating that the lack of an Airy crustal root is a regional feature of the topographically high eastern ranges. Simple calculations demonstrate that either a local mantle density anomaly directly beneath the eastern Peninsular Ranges or flexural transfer of extension-related loads originating in the Gulf Extensional Province could support the topographic load of the eastern ranges. The former could be achieved, for example, by a 3% upper mantle density reduction over 65 km vertical extent. The latter mechanism would require that the crust, despite being subjected to large amounts of extensional strain, maintains a significant amount of elastic strength, equivalent to roughly 5 km elastic thickness. Available observations do not permit us to exclude either mechanism, and we conclude that support of the Peninsular Ranges topography may be achieved through a combination of flexural support and lateral density variations in the crust and/or upper mantle.

Appendix A

The equation governing vertical (positive downward) deflection w of a thin elastic plate (representing lithosphere with crustal density ρ_c, mantle density ρ_m, and flexural rigidity D) over a fluid substrate (with mantle density ρ_m) is given by *Turcotte and Schubert* [1982, p. 122]. Assuming that there is an applied vertical load q, which depends only on one coordinate x, and that $q(x)$ is balanced by hydrostatic and flexural restoring forces, this equation is

$$D\,\frac{d^4w}{dx^4} + g(\rho_m - \rho_c)w = q(x) \qquad \text{(A1)}$$

(g is the gravitational acceleration). In our application of (A1), the load $q(x)$ includes the term $q_1(x) = g\rho_c h(x)$, where $h(x)$ is the height of surface topography above sea level, and the term $q_2(x)$ which represents other vertical loads such as crustal mass addition or removal and lateral variations in mantle density.

We take x to increase eastward along the cross section C-C′ of Figure 3, with $x = 0$ at the Main Gulf Escarpment (taken as the point where the cross section intersects the Sierra San Pedro Mártir Fault). The topographic load q_1 on the Baja peninsula is derived by setting $h(x)$ to the surface elevation along the cross section, and q_1 is set to zero over the Gulf of California. A vertical load related to gulf extension, q_2, is assumed (for the illustrative purposes of this idealized calculation) to be (1) confined to $x > 0$, i.e., to east of the Main Gulf Escarpment separating the Peninsular Ranges from the Gulf Extensional Province, so that $q_2 = 0$ for $x < 0$; (2) uniform on $x > 0$, i.e., $q_2 =$ const for $x > 0$; and (3) scaled to deflect the plate upward by $\delta h = 19$ km in the limit $x \gg [D/g(\rho_m - \rho_c]^{1/4}$ (i.e., for positions which lie east of the Main Gulf Escarpment by a distance large compared with the natural wavelength for flexure). Therefore, $q_2 = -g(\rho_m - \rho_c)\delta h H(x)$, where H is the Heaviside step function. This amount of assumed upward deflection in the Gulf province corresponds to the difference between our assumed unloaded (i.e., sea level topography) peninsular crustal thickness of 34 km and our inferred gulf crustal thickness of ~15 km. The uniform, negative (upward) load confined to $x > 0$ may be viewed as a schematic representation of extension-related effects including rebound from mass removal (e.g., by brittle faulting and ductile transport, net of replacement by seawater and sediments), uplift of the geothermal gradient, and presence of enhanced mantle buoyancy sources.

We Fourier transform and solve (A1) (transforming $q(x)$ numerically) and then recover $w(x)$ by numerically inverse transforming the solution. The assumed mantle and crustal densities are 3300 and 2800 km/m^3, respectively. We express flexural rigidity in terms of an effective elastic thickness T, i.e., $D = \mu T^3/6(1 - v)$, where μ (3×10^{10} Pa) is the shear modulus and v (0.25) is Poisson's ratio.

Acknowledgments. We wish to express our gratitude to the technical staff of CICESE for their help during the field work. Some of the instrumentation was provided by the Southern California Earthquake Center (SCEC) and the IRIS PASSCAL program (NSF Cooperative Agreement EAR-9529992), and we thank Jim Fowler (IRIS) and Aaron Martin (SCEC) for their assistance. We benefited greatly from the review comments provided by Vera Schlindwein, Martha Savage, and Walter Mooney. This project received support from the Cecil and Ida Green Foundation (at the University of California, San Diego), the Rollin and Caroline Eckis Endowment (at San Diego State University), and SCEC. SCEC is funded by NSF Cooperative Agreement EAR-8920136 and USGS Cooperative Agreements 14-08-0001-A0899 and 1434-HQ-97AG01718. This is SCEC contribution 521.

References

Allison, E. C., Geology of areas bordering Gulf of California, in *Marine Geology of the Gulf of California*, edited by T. H. van Andel and G. G. Shor Jr., *AAPG Mem.*, *3*, 3–29, 1964.

Ammon, C. J., G. E. Randall, and G. Zandt, On the nonuniqueness of receiver function inversions, *J. Geophys. Res.*, *95*, 15,303–15,318, 1990.

Astiz, L., R. Castro, J. Eakins, F. L. Vernon, C. Rebollar, S. M. Day, and J. N. Brune, The North Baja Transect (NBT): A seismic experiment in our backyard, paper presented at 10th Annual IRIS Workshop, Santa Cruz, Calif., 1998.

Axen, G., Extensional segmentation of the Main Gulf Escarpment, México and United States, *Geology*, *23*, 515–518, 1995.

Bechtel, T. D., D. W. Forsyth, V. L. Sharpton, and R. A. F. Grieve, Variations in effective elastic thickness of the North American lithosphere, *Nature*, *343*, 636–638, 1990.

Brown, L. G., Recent fault scarps along the eastern escarpment of the Sierra San Pedro Mártir, Baja California, M.S. thesis, San Diego State Univ., San Diego, Calif., 1978.

Burchfiel, B. C., D. S. Cowan, and G. A. Davis, Tectonic overview of the Cordilleran orogen in the western United States, in *The Geology of North America*, vol. G3, *The Cordilleran Orogen, Conterminous United States*, edited by B. C. Burchfiel et al., pp. 407–482, Geol. Soc. of Am., Boulder, Colo., 1992.

Cassidy, J. F., Numerical experiments in broadband receiver function analysis, *Bull. Seismol. Soc. Am.*, *82*, 1453–1474, 1992.

Dokka, R. K., and R. H. Merriam, Late Cenozoic extension of northeastern Baja California, *Geol. Soc. Am. Bull.*, *93*, 371–378, 1982.

Efron, B., *The Jackknife, the Bootstrap and Other Resampling Plans*, Soc. of Ind. and Appl. Math., Philadelphia, Pa., 1982.

Egan, S. S., The flexural isostatic response of the lithosphere to extensional tectonics, *Tectonophysics*, *202*, 291–308, 1992.

Fliedner, M. M., S. Rupert, and SSDC Working Group, Three-dimensional structure of the southern Sierra Nevada from seismic fan profiles and gravity modeling, *Geology*, *24*, 367–370, 1996.

Fuis, G. S., W. D. Mooney, J. H. Healy, G. A. McMehan, and W. J. Lutter, Crustal structure of the Imperial Valley region, *U.S. Geol. Surv. Prof. Pap.*, *1254*, 25–49, 1982.

Gastil, R. G., Prebatholithic history of peninsular California, in *The Prebatholithic Stratigraphy of Peninsular California*, edited by R. G. Gastil and R. H. Miller, *Spec. Pap. Geol. Soc. Am.*, *279*, 145–156, 1993.

Gastil, R. G., R. P. Phillips, and E. C. Allison, Reconnaissance geology of the State of Baja California, México, *Mem. Geol. Soc. Am.*, *140*, 170 pp., 1975.

Henyey, T. L., and J. L. Bischoff, Tectonic elements of the northern part of the Gulf of California, *Geol. Soc. Am. Bull.*, *84*, 315–330, 1973.

Ichinose, G. A., S. Day, H. Magistrale, T. Prush, F. Vernon, and A. Edelman, Crustal thickness variations beneath the Peninsular

Ranges, southern California, *Geophys. Res. Lett.*, *23*, 3095–3098, 1996.

Jones, C. H., and R. A. Phinney, Seismic structure of the lithosphere from teleseismic converted arrivals at small arrays in the southern Sierra Nevada and vicinity, California, *J. Geophys. Res.*, *103*, 10,065–10,090, 1998.

Jones, C. H., H. Kanamori, and S. W. Roecker, Missing roots and mantle "drips": Regional P_n and teleseismic arrival times in the southern Sierra Nevada and vicinity, California, *J. Geophys. Res.*, *99*, 4567–4601, 1994.

Kennett, B. N. L., and E. R. Engdahl, Travel times for global earthquake location and phase identification, *Geophys. J. Int.*, *106*, 429–465, 1991.

Lachenbruch, A. H., J. H. Sass, and S. P. Galanis, Jr., Heat flow in southernmost California and the origin of the Salton trough, *J. Geophys. Res.*, *90*, 6709–6736, 1985.

Langston, C. A., Structure under Mount Rainier, Washington, inferred from teleseismic body waves, *J. Geophys. Res.*, *84*, 4749–4762, 1979.

Lewis, C. J., and J. M. Stock, Late Miocene to Recent transtensional tectonics in the Sierra San Fermín, northeastern Baja California, México, *J. Struct. Geol.*, *20*, 1043–1063, 1998.

Lewis, J. L., S. M. Day, H. Magistrale, J. Eakins, and F. Vernon, Regional crustal thickness variations of the Peninsular Ranges, southern California, *Geology*, *28*, 303–306, 2000.

Lonsdale, P., Geology and tectonic history of the Gulf of California, in *The Geology of North America*, vol. N, *The Eastern Pacific Ocean and Hawaii*, edited by E. L. Winterer et al., pp. 499–521, Geol. Soc. of Am., Boulder, Colo., 1989.

Magistrale, H., Seismotectonics and crustal velocities in the Imperial Valley, California (abstract), *Eos Trans. AGU.*, *80*(46), Fall Meet. Suppl., F715, 1999.

Magistrale, H., and C. Sanders, *P* wave image of the Peninsular Ranges batholith, southern California, *Geophys. Res. Lett.*, *22*, 2549–2552, 1995.

Nava, F. A., and J. N. Brune, An earthquake-explosion reversed refraction line in the Peninsular Ranges of southern California and Baja California Norte, *Bull. Seismol. Soc. Am.*, *72*, 1195–1206, 1982.

Oskin, M., and J. Stock, Separation of Baja California from North America: New constraints on timing and total displacement (abstract), *Geol. Soc. Am. Abstr. Programs*, *31*, A294, 1999.

Owens, T. J., G. Zandt, and S. R. Taylor, Seismic evidence for an ancient rift beneath the Cumberland Plateau, Tennessee: A detailed analysis of broadband teleseismic *P* waveforms, *J. Geophys. Res.*, *89*, 7783–7795, 1984.

Parsons, T., and J. McCarthy, Crustal and upper mantle velocity structure of the Salton trough, southeastern California, *Tectonics*, *15*, 456–471, 1996.

Phillips, R. P., Seismic refraction studies in Gulf of California, in *Marine Geology of the Gulf of California*, edited by T. H. van Andel and G. G. Shor Jr., *AAPG Mem.*, *3*, 90–125, 1964.

Sanchez-Zamora, O., P. Dougin, R. W. Couch, and G. E. Ness, Magnetic anomalies of the northern Gulf of California: Structural and thermal interpretations, in *The Gulf and Peninsular Province of the Californias*, edited by J. P. Dauphin and B. R. T. Simoneit, *AAPG Mem.*, *47*, vol. 1, 377–401, 1991.

Scott, J. S., Microearthquake studies in the Anza seismic gap, Ph.D. thesis, Univ. of Calif., San Diego, 1992.

Silver, L. T., and B. W. Chappell, The Peninsular Ranges batholith: An insight into the evolution of the Cordilleran batholiths of southwestern North America, *Trans. R. Soc. Edinburgh*, *Earth Sci.*, *79*, 105–121, 1988.

Silver, L. T., H. P. Taylor, and B. W. Chappell, Some petrological, geochemical, and geochronological observations of the Peninsular Ranges batholith near the international border of the U.S.A. and México, in *Mesozoic crystalline rocks: Peninsular Ranges Batholith and Pegmatites and Point Sal Ophiolite*, edited by P. Abbott and V. Todd, pp. 83–110, Geol. Soc. of Am., Boulder, Colo., 1979.

Slyker, R. G., Jr., Geologic and geophysical reconnaissance of the Valle de San Felipe region, Baja California, México, M.S. thesis, San Diego State Univ., Calif., 1970.

Stock, J. M., and K. V. Hodges, Miocene to recent structural development of an extensional accommodation zone, northeastern Baja California, México, *J. Struct. Geol.*, *12*, 315–328, 1990.

Stock, J. M., A. Martín-Barajas, F. Suárez-Vidal, and M. M. Miller, Miocene to Holocene extensional tectonics and volcanic stratigraphy of northeastern Baja California, México, in *Geological Excursions in Southern California and México*, edited by M. J. Walawender and B. B. Hanan, pp. 44–67, Geol. Soc. of Am., Boulder, Colo., 1991.

ten Brink, U. S., J. Zhang, T. M. Brocher, D. A. Okaya, K. D. Klitgord, and G. S. Fuis, Geophysical evidence for the evolution of the California Inner Continental Borderland as a metamorphic core complex, *J. Geophys. Res.*, *105*, 5835–5857, 2000.

Thomson, C. N., and G. H. Girty, Early Cretaceous intra-arc ductile strain in Triassic-Jurassic and Cretaceous continental margin arc rocks, Peninsular Ranges, California, *Tectonics*, *13*, 1108–1119, 1994.

Turcotte, D. L., and G. Schubert, *Geodynamics: Applications of Continuum Physics to Geological Problems*, 450 pp., John Wiley, New York, 1982.

Wernicke, B., et al., Origin of high mountains in the continents: The southern Sierra Nevada, *Science*, *271*, 190–193, 1996.

Zhu, L., and H. Kanamori, Moho depth variation in southern California from teleseismic receiver functions, *J. Geophys. Res.*, *105*, 2969–2980, 2000.

L. Astiz, CTBTO PrepCom, P.O. Box 1250:A-1400 Vienna, Austria. (luciana.astiz@ctbto.org)

J. N. Brune, Seismological Laboratory, University of Nevada at Reno, Reno, NV 89557. (brune@seismo.unr.edu)

R. R. Castro and Cecilio Rebollar, División Ciencias de la Tierra, Centro de Investigación Científica y de Educación Superior de Ensenada, Ensenada, Baja California, México. (raul@cicese.mx)

S. M. Day and H. Magistrale, Department of Geological Sciences, San Diego State University, 5500 Campanile Drive, San Diego, CA 92182. (day@moho.sdsu.edu)

J. Eakins and F. L. Vernon, Institute of Geophysics and Planetary Physics, University of California, San Diego, La Jolla, CA 92093. (flvernon@ucsd.edu)

J. L. Lewis, Chevron North America Exploration and Production, 935 Gravier St., New Orleans, LA 70112. (jnnl@chevron.com)

(Received June 28, 2000; revised January 22, 2001;
accepted March 24, 2001.)